CrossMark

ORIGINAL PAPER

Improving the performance of a nonlinear boiler–turbine unit via bifurcation control of external disturbances: a comparison between sliding mode and feedback linearization control approaches

Hamed Moradi · **Mohammad Hossein Abbasi** · **Hossein Moradian**

Abstract Boiler–turbine units may show quasiperiodic behavior due to the bifurcation occurrence in the presence of harmonic disturbances. In this study, a multi-input–multi-output nonlinear dynamic model of a boiler–turbine unit is considered. Drum pressure, electric output, and fluid density are the state variables and adjusted at the desired values by manipulation of the input variables. Control inputs are the valve positions for fuel, steam and feed-water flow rates. To improve the quasiperiodic behavior of the system and bifurcation control in tracking problem, two controllers are designed: feedback linearization control and nonlinear sliding mode control (SMC). The feedback linearization controller is designed based on the linearized dynamics. Dynamic response of the system in tracking of four different desired trajectories is examined. SMC controller acts more efficiently in suppression of harmonic perturbations and consequently bifurcation control. Appropriate tracking performance is observed for the drum pressure, electric output, fluid density and drum water level in both cases. Control efforts' magnitudes in both controllers are almost similar. However, sliding mode controller vanishes the quasiperiodic solutions more successfully and leads to a more smooth response with less overshoots and less corresponding control efforts.

H. Moradi (✉) · M. H. Abbasi · H. Moradian
Centre of Excellence in Design, Robotics and Automation
(CEDRA), School of Mechanical Engineering, Sharif
University of Technology, Tehran 11155-9567, Iran
e-mail: hamedmoradi@sharif.edu

1 Introduction

Boiler–turbine is one of the most important components in power plants. Due to its dynamic interaction with different equipment, it has a complex nonlinear dynamic model. During the power plant operation, variables such as steam pressure, electric output, fluid density, and drum water level should be maintained at their desired values [1,2].

Different dynamic models have been proposed with the help of neural networks [3], using data logs and parameter estimation [4], applying T–S fuzzy method [5] and fuzzy-neural network methods [6]. Moreover, many works have been done on dynamic modelling of this unit based on simplification of nonlinear models of boiler–turbine units [7], parameter estimation [8], system identification using neural networks [9], data logs [10], and fuzzy auto-regressive moving average model [11]. Also, nonlinear dynamics of the unit was investigated through the concepts of bifurcation and limit cycles behavior [12]. Moreover, state space equations of a model for a hydro-turbine system considering surge tank effects were introduced and critical points of Hopf bifurcation were obtained [13].

In addition to dynamic modelling, various control approaches have been applied for the boiler or boiler–

turbine units. These controllers helped the boiler or boiler–turbine units to perform appropriately. Linear optimal regulators [14,15], decoupling controller [16], multivariable long-range predictive control based on local model networks [17], fuzzy model predictive control based on genetic algorithm [18], fuzzy based control systems for thermal power plants [19,20] and neuro-fuzzy network modelling and PI control of a steam-boiler system [21] have been investigated. In addition, linear control theories such as gain scheduled optimal control have been used [22].

Moreover, backstepping-based nonlinear adaptive control [23], adaptive dynamic matrix control with fuzzy-interpolated step-response model [24], sliding mode and H_∞ robust controllers [2,25–28] and a comparison between them [2,27] have been applied for robust performance of the unit. Furthermore, gain scheduling and feedback linearization controllers in tracking problem [29] and a control regulator based on feedback linearization [12] have been designed for the bifurcation control.

To the best of our knowledge, most of previous studies have been devoted to simplification of the complex nonlinear dynamic system and controller design accordingly. Due to this simplification, the designed controllers may lead to the aggressive response of output variables and also increase in energy consumption.

Harmonic perturbations essentially occur for the power grid. In this study, tracking of the desired commands is studied in the presence of such perturbations. Four desired tracking objectives are considered as desired set-paths. In the previous works, only linear controllers are proposed for tracking in the presence of perturbations. In this paper, two controllers are designed: one is applied on the nonlinear complex model, and the other is applied on the linearized simplified model. System responses of these two controllers are compared regarding tracking of the desired commands, bifurcation control and consequently changing the unstable quasiperiodic solutions into the stable periodic ones. Moreover, the behavior of control efforts for tracking of the desired paths is also investigated.

2 Nonlinear dynamic model of the boiler–turbine unit

A water-tube boiler is considered as the case study for this study. The whole process of this unit is shown
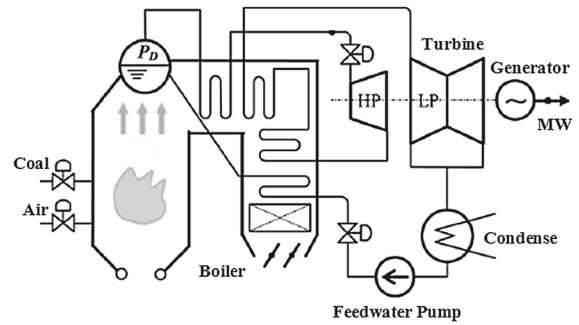
Fig. 1 Schematic of a boiler–turbine unit [29]

in Fig. 1 schematically [30]. As a real case study, all simulations in this study are applied on the nonlinear dynamic model of a boiler–turbine unit presented by Bell and Astrom [31]. Parameters of this model were estimated from experimental data related to the 160 MW Synvendska Kraft AB Plant in Malmo, Sweden. Output variables are indicated by y_1 for drum pressure (kg f/cm^2), y_2 for electric output (MW) and y_3 for drum water level (m) shown in Figure 2 [22]. Input variables are denoted by u_1, u_2, and u_3 for the valves position of the fuel flow, steam control, and feed-water flow, respectively. Dynamic equations of this unit are described as the followings [31]:

$$\dot{x}_1 = -\alpha_1 u_2 x_1^{9/8} + \alpha_2 u_1 - \alpha_3 u_3$$
$$\dot{x}_2 = (\beta_1 u_2 - \beta_2) x_1^{9/8} - \beta_3 x_2$$
$$\dot{x}_3 = [\gamma_1 u_3 - (\gamma_2 u_2 - \gamma_3) x_1]/\gamma_4 \qquad (1)$$

where x_1, x_2, x_3 denotes drum pressure (kg f/cm^2), electric output (MW), and the fluid density (kg/m^3), respectively. Also coefficients $\alpha_i, \beta_i, \gamma_j$ $i = 1 \ldots 3$, $j = 1 \ldots 4$ are listed in Table 1. Drum water level (y_3) is given in terms of the steam quality a_{cs} and evaporation rate q_e (kg/s) as:

$$y_3 = 0.05 \left(0.13073 x_3 + 100 a_{cs} + \frac{q_e}{9} - 67.975 \right) \quad (2)$$

where

$$a_{cs} = \frac{(1 - 0.001538 x_3)(0.8 x_1 - 25.6)}{x_3 (1.0394 - 0.0012304 x_1)}$$
$$q_e = (0.854 u_2 - 0.147) x_1 + 45.59 u_1$$
$$\quad - 2.514 u_3 - 2.096 \qquad (3)$$

Fig. 2 Multivariable model of the boiler–turbine unit and structure of the closed-loop control system
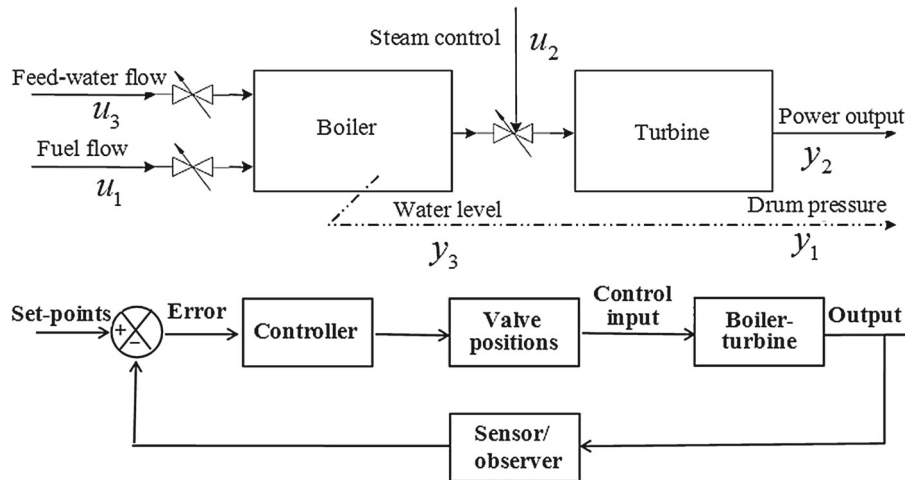
Table 1 Dynamic coefficients of the boiler–turbine model by Bell and Astrom [30]

$\alpha_1 = 0.0018$	$\beta_1 = 0.073$	$\gamma_1 = 141$
$\alpha_2 = 0.9$	$\beta_2 = 0.016$	$\gamma_2 = 1.1$
$\alpha_3 = 0.15$	$\beta_3 = 0.1$	$\gamma_3 = 0.19$
		$\gamma_4 = 85$

and considering the actuator limitations, control inputs and their rates are limited as below [30]:

$$0 \leq u_i \leq 1$$
$$-0.007 \leq \dot{u}_1 \leq 0.007$$
$$-2 \leq \dot{u}_2 \leq 0.02$$
$$-0.05 \leq \dot{u}_3 \leq 0.05 \quad (i = 1, 2, 3) \qquad (4)$$

Table 2 gives some typical operating points of the Bell and Astrom model where the nominal model coincides with the operating point #4 [31].

In order to include more reality to the model, real harmonic disturbances in state variables are considered, for instance, as:

$$\Delta x_1 = 10 \sin 0.021t; \; \Delta x_2 = 6 \sin 0.021t;$$
$$\Delta x_3 = 40 \sin 0.021t \qquad (5)$$

The magnitudes of disturbances are chosen arbitrarily around 10 % of the magnitudes of the nominal operating point #4 with arbitrary period of 5 min. Thus, every state vector component $x_i(t)$ in Eq. (1) is replaced by $x_i(t) + \Delta x_i(t)$.

3 Controller design

In very limited number of previous studies, only the linear control approaches have been implemented on this system for bifurcation analysis. In this paper, results of a nonlinear control and a linear control are compared. For the nonlinear control approach, sliding mode con-

Table 2 Typical operating points of Bell and Astrom model [30]

	#1	#2	#3	#4	#5	#6	#7
x_1^0	75.6	86.4	97.2	108	118.8	129.6	140.4
x_2^0	15.27	36.65	50.52	66.65	85.06	105.8	128.9
x_3^0	299.6	342.4	385.2	428	470.8	513.6	556.4
u_1^0	0.156	0.209	0.271	0.34	0.418	0.505	0.6
u_2^0	0.483	0.552	0.621	0.69	0.759	0.828	0.897
u_3^0	0.183	0.256	0.34	0.433	0.543	0.663	0.793
y_3^0	−0.97	−0.65	−0.32	0	0.32	0.64	0.98

troller (SMC) and for the linear one, feedback lineariza-
tion method (FLM) are implemented. It is assumed that
all state variables in the model are available for con-

struction of the feedback control law, either by direct
measurement or by using a state observer. For more
details, one can refer to the previous research [32].

Fig. 3 Desired set-paths for tracking objectives in switching between the operating points #1 to #7 for **a** a sequence of steps, **b** ramps, **c** step-ramps and **d** sinusoidal signal
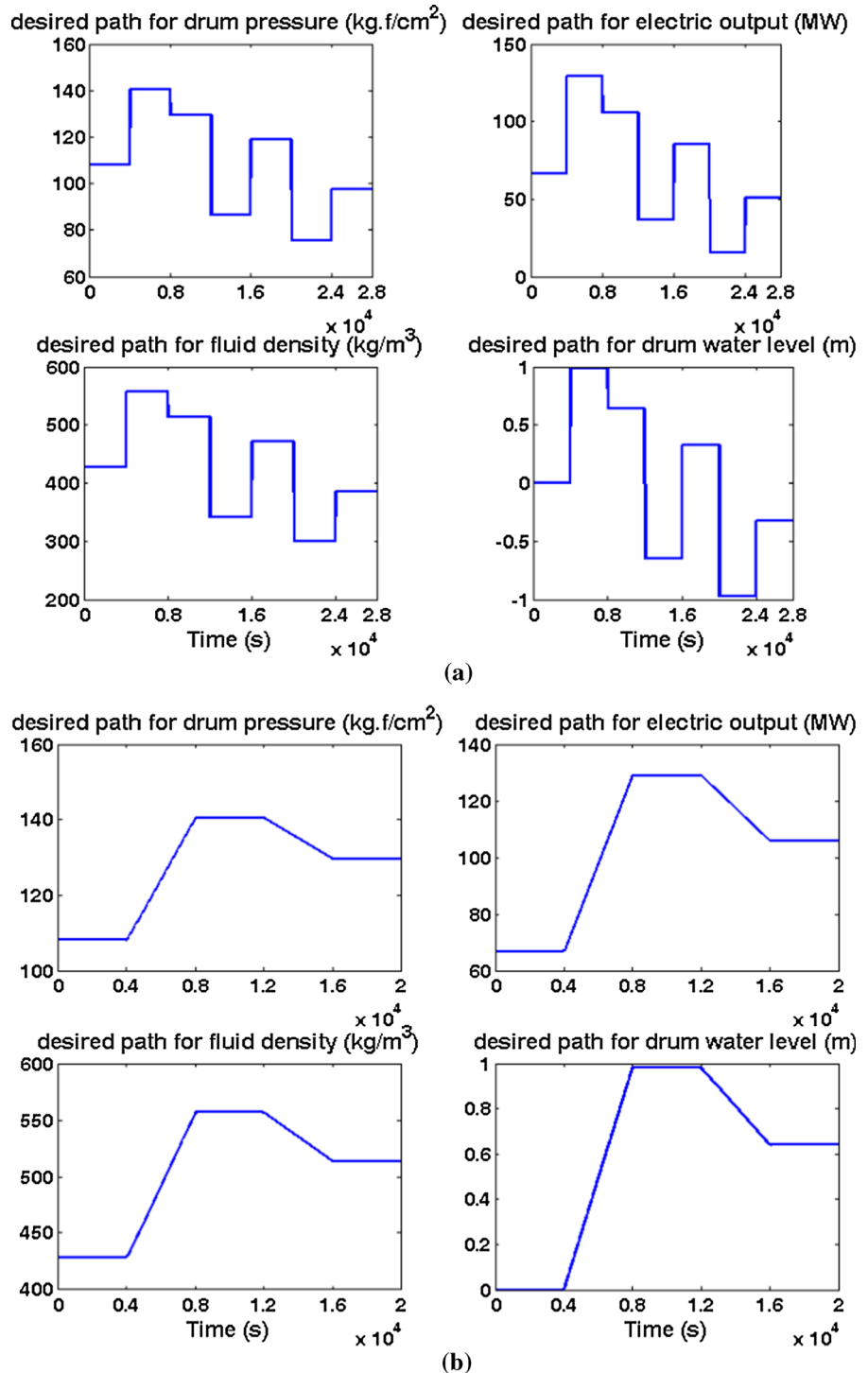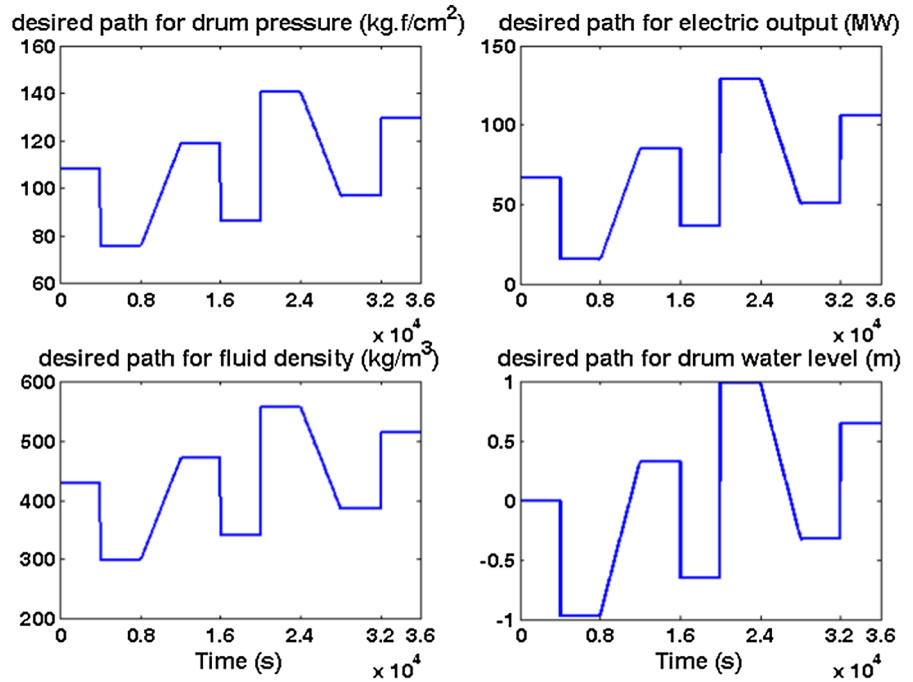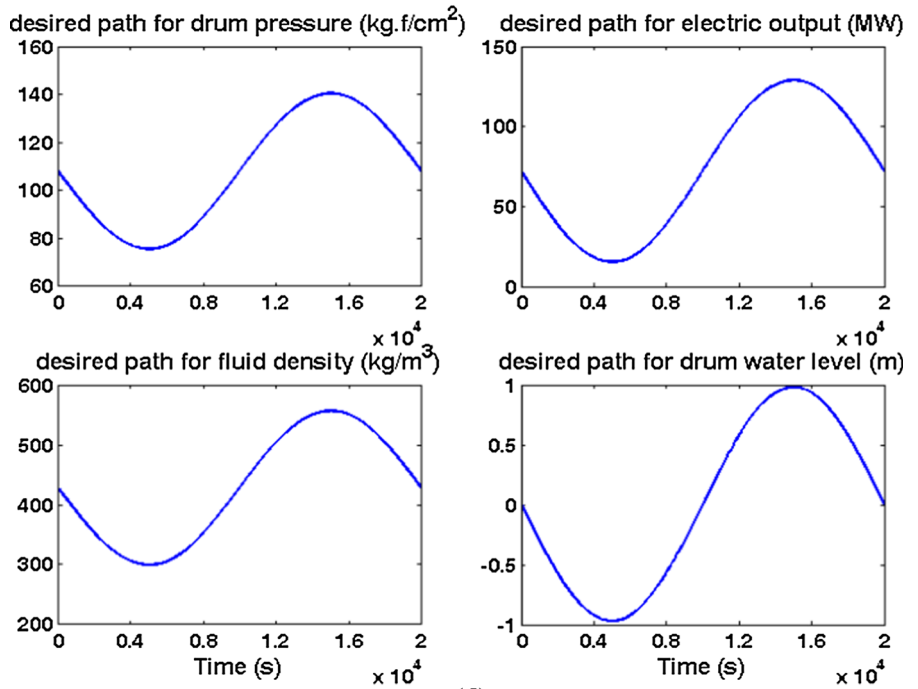
Fig. 3 continued
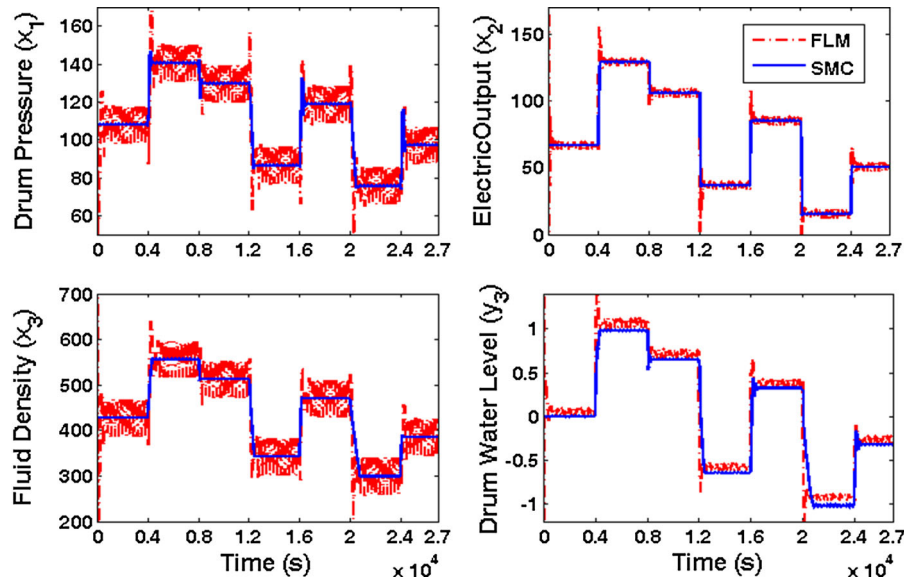

(c)


(d)

Fig. 4 Time response of the drum pressure (kg f/cm^2), electric output (MW), fluid density and drum water level in tracking a sequence of steps (case 'a' of Fig. 4) after implementation of sliding mode controller (*solid blue line*) and feedback linearization method (*dashed red line*); in the presence of Hopf bifurcation. (Color figure online)

Fig. 5 Periodic and quasi-periodic orbits of drum pressure (kg f/cm^2) in tracking a sequence of steps (case 'a'); after implementation of sliding mode controller (*solid blue line*) and feedback linearization method (*dashed red line*). (Color figure online)
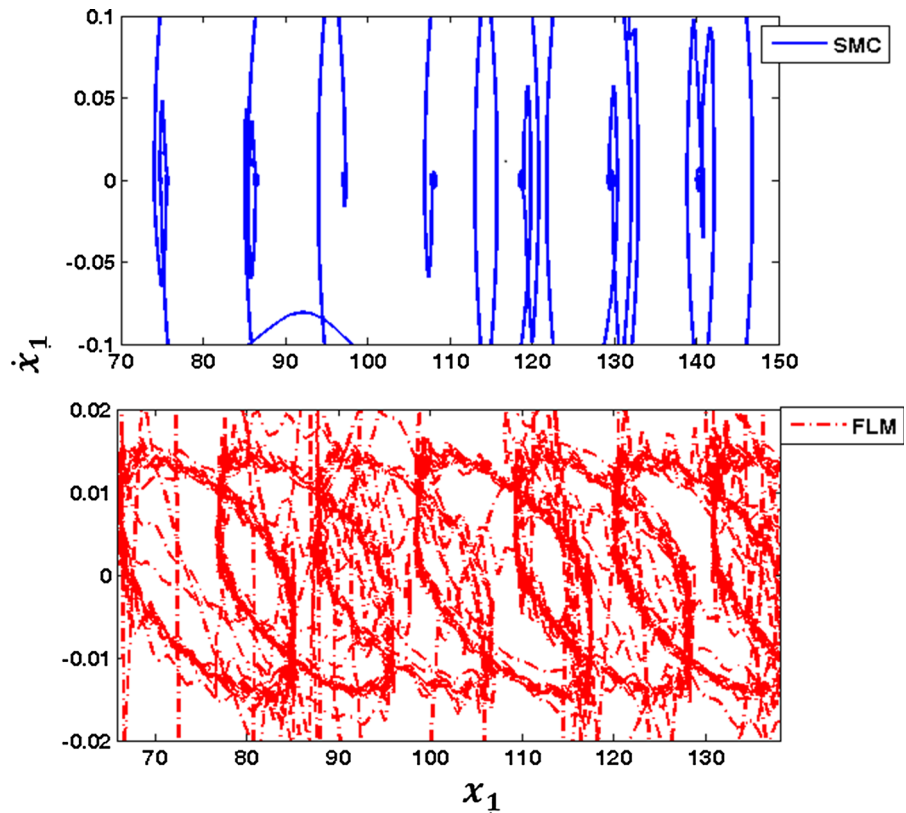
3.1 Nonlinear control using the sliding mode control approach

In this section, nonlinear dynamics of the boiler–turbine is considered. This method is suitable for control of nonlinear systems [33]. However, in previous studies, the controllers were designed based on the linearized model [12,29].

Sliding mode controller is one of approaches used for the robust control of different mechanical sys-

Fig. 6 Time response of the required fuel flow rate, u_1, steam flow rate, u_2, and feed-water flow rate, u_3 for the Hopf bifurcation control in tracking a sequence of steps (case 'a'); after implementation of sliding mode controller (*solid blue line*) and feedback linearization method (*dashed red line*). (Color figure online)
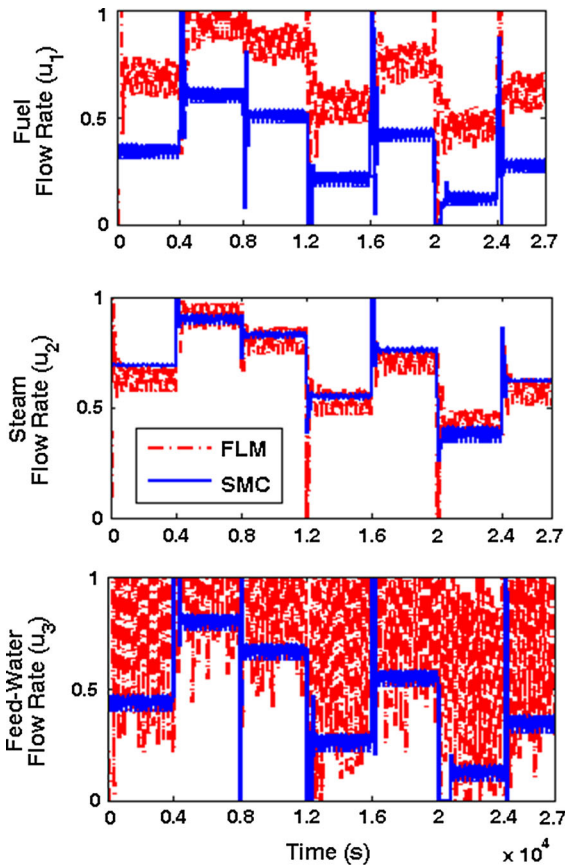
tems [2,27]. In this method, the nth-order problem is replaced by n equivalent first-order problems. Consider the nonlinear dynamic system with multiple inputs as:

$$\dot{x} = f(x, t) + g(x, t)u \tag{6}$$

where x and u are the state vector and the control input, respectively. $f(x, t)$ and $g(x, t)$ are the nonlinear functions of time and states. These functions may have uncertainties and even unmodelled dynamics; however, they are bounded. A sliding surface vector can be defined as:

$$s(x, t) = e(t) = [e_1 \quad e_2 \quad e_3] \tag{7}$$

where $e(t) = x(t) - x_d(t)$ is the tracking error, $x_d(t)$ is the desired state to be tracked. To guarantee Lyapunov stability condition, the control law u of Eq. (6) must be selected such that:

$$\frac{1}{2}\frac{d}{dt}s^2 = s\dot{s} \leq -\eta |s| \tag{8}$$

where η is a positive constant [for simplicity, $s(y, t)$ is denoted by s]. Equation (8) mentions that the squared distance to the surface decreases along all system trajectories, and thus it makes the trajectories to move toward the origin. If $x(t = 0) \neq x_d(t = 0)$, sliding surface s can be reached in a finite time smaller than $|s(t = 0)| /\eta$. In order $x(t)$ to track $x_d(t)$, sliding surface s is defined as Eq. (7). The time derivative of s is

$$\dot{s} = \dot{x} - \dot{x}_d = f(x, t) + g(x, t)u - \dot{x}_d \tag{9}$$

The approximation $\hat{u}$ of a continuous control law that would achieve $\dot{s} = 0$ is:

$$\hat{u} = \bar{g}^{-1}(x, t)\left[\dot{x}_d - \bar{f}(x, t)\right] \tag{10}$$

where $\bar{g}(x, t)$ and $\bar{f}(x, t)$ are the nominal values associated with $g(x, t)$ and $f(x, t)$. In spite of the uncertainty and unmodelled dynamics associated with the model, to satisfy the sliding condition, a discontinuous term across the surface $s = 0$ is added as:

$$u = \hat{u} - g^{-1}(x, t)\left[K_1\text{sgn}(s_1) \quad K_2\text{sgn}(s_2) \quad K_3\text{sgn}(s_3)\right]^T \tag{11}$$

where sgn is the sign function. It can be shown that by assigning K_1, K_2 and K_3 large enough, condition in Eq. (8) will be satisfied. To eliminate control signal chattering, the control discontinuity must be smoothed in a thin boundary layer around the switching surface. Thus, the sign function is replaced by a saturation function, so the control input u is modified to

$$u = \hat{u} - \bar{g}^{-1}(x, t)$$
$$\times \left[K_1\text{sat}(s_1/\xi_1) \quad K_2\text{sat}(s_2/\xi_2) \quad K_3\text{sat}(s_3/\xi_3)\right]^T$$
$$\text{sat}(s/\xi) = \begin{cases} s/\xi & |s| \leq \xi \\ \text{sgn}(s) & \text{otherwise} \end{cases} \tag{12}$$

where ξ is the thickness of boundary layer. Using control law of Eq. (12) guarantees the tracking and generally is valid for the all trajectories starting inside the boundary layer.

Fig. 7 Time response of the drum pressure (kg f/cm^2), electric output (MW), fluid density and drum water level in tracking a sequence of ramps (case 'b' of Fig. 3) after implementation of sliding mode controller (*solid blue line*) and feedback linearization method (*dashed red line*), in the presence of Hopf bifurcation. (Color figure online)
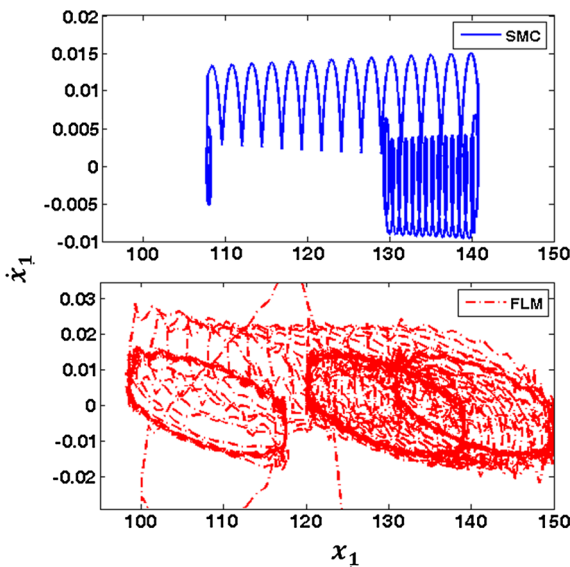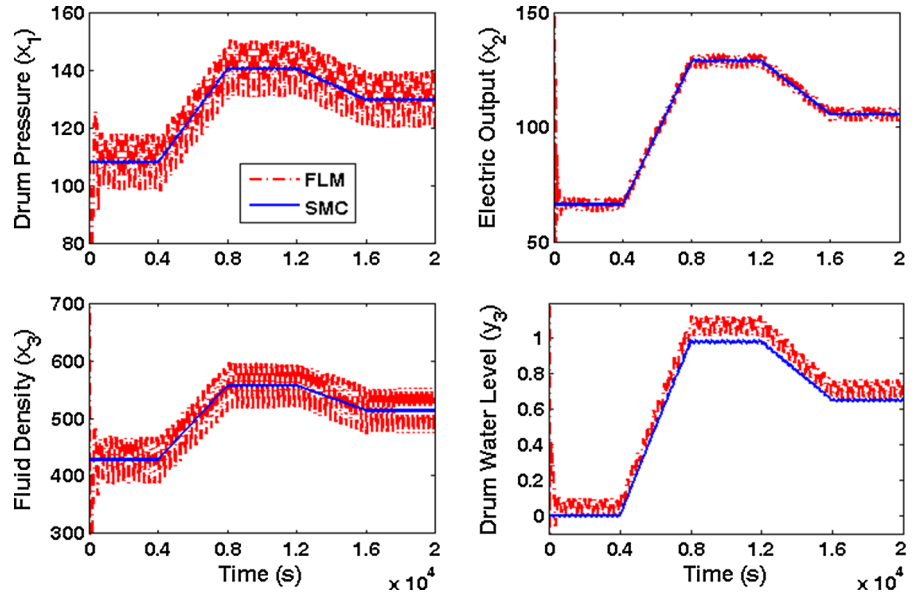
Fig. 8 Periodic and quasi-periodic orbits of drum pressure (kg f/cm^2) in tracking a sequence of ramps (case 'b'), after implementation of sliding mode controller (*solid blue line*) and feedback linearization method (*dashed red line*). (Color figure online)

Theorem 1 *Consider the plant described by Eq.(6). If the control law by Eq. (12) is applied on the plant, the tracking error converges to zero. K_1, ξ_1, K_2, ξ_2 and K_3, ξ_3 are the constant design parameters.*

Proof In order to prove the stability of the control system, a positive-definite Lyapunov function is defined as below:
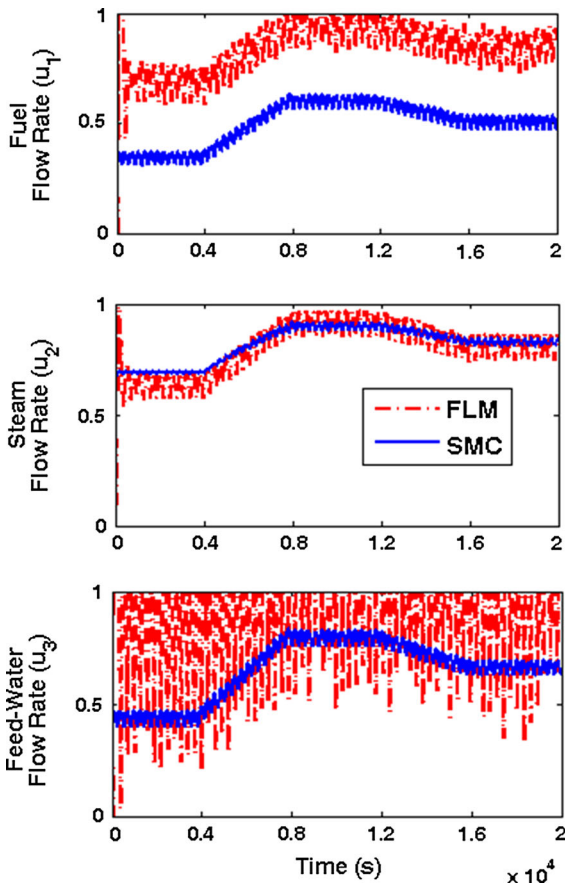
$$V = \frac{1}{2}\left(e_1^2 + e_2^2 + e_3^2\right) = \frac{1}{2}s^T s \tag{13}$$

Time derivative of Lyapunov function is obtained as:

$$\begin{aligned} \dot{V} &= e_1\dot{e}_1 + e_2\dot{e}_2 + e_3\dot{e}_3 = s^T\dot{s} \\ &= s^T\left[f(x,t) + g(x,t)u - \dot{x}_d\right] \end{aligned} \tag{14}$$

Replacing the control law by Eq. (12) into Eq. (14), yields:

Fig. 9 Time response of the required fuel flow rate, u_1, steam flow rate, u_2, and feed-water flow rate, u_3 for the Hopf bifurcation control in tracking a sequence of ramps (case 'b'); after implementation of sliding mode controller (*solid blue line*) and feedback linearization method (*dashed red line*). (Color figure online)

3.2 Linear control using the feedback linearization method

Formulation of the controller design using feedback linearization approach was presented in the previous research [12] (also, it is presented briefly in "Appendix"). In this section, the linear model of the system is presented.

Dynamic model given by Eq. (1) is considered. To maintain the system around each operating point of Table 2 at the state vector $\bar{x}^0 = [x_1^0 \ x_2^0 \ x_3^0]$, a constant input vector $\bar{u}^0 = [u_1^0 \ u_2^0 \ u_3^0]$ must be imposed. For math simplicity, let's define the new variables as:

$$\xi_1 = x_1^0, \quad \xi_2 = x_2^0, \quad \xi_3 = x_3^0$$
$$\eta_1 = u_1^0, \quad \eta_2 = u_2^0, \quad \eta_3 = u_3^0 \tag{16}$$

By linearizing the Eq. (1) around any operating points of Table 2, one can conclude:

$$\dot{\bar{x}}_\delta = A(\xi_i, \eta_i)\bar{x}_\delta + B(\xi_i, \eta_i)\bar{u}_\delta \quad i = 1, 2, 3$$
$$\bar{x}_\delta = \bar{x} - \bar{x}^0, \bar{u}_\delta = \bar{u} - \bar{u}^0 \tag{17}$$

where

$$A(\xi_i, \eta_i) = \begin{bmatrix} -1.125\alpha_1\eta_2\xi_1^{1/8} & 0 & 0 \\ 1.125(\beta_1\eta_2 - \beta_2)\xi_1^{1/8} & -\beta_3 & 0 \\ -\frac{1}{\gamma_4}(\gamma_2\eta_2 - \gamma_3) & 0 & 0 \end{bmatrix};$$

$$B(\xi_i, \eta_i) = \begin{bmatrix} \alpha_2 & -\alpha_1\xi_1^{9/8} & -\alpha_3 \\ 0 & \beta_1\xi_1^{9/8} & 0 \\ 0 & -\frac{\gamma_2}{\gamma_4}\xi_1 & \frac{\gamma_1}{\gamma_4} \end{bmatrix} \tag{18}$$

In state feedback control scheme, to achieve the desired locations of closed-loop control system and consequently desired performance of the system, the control vector $\bar{u}_\delta$ is constructed as:

$$\dot{V} = s^T \left(f(x,t) + g(x,t)\bar{g}^{-1}(x,t)\left(\dot{x}_d - \bar{f}(x,t) - \left[K_1\text{sat}(s_1/\xi_1) \ K_2\text{sat}(s_2/\xi_2) \ K_3\text{sat}(s_3/\xi_3) \right]^T\right) - \dot{x}_d \right)$$

$$\dot{V} = s^T \left(\begin{matrix} \left(f(x,t) - g(x,t)\bar{g}^{-1}(x,t)\bar{f}(x,t)\right) + \dot{x}_d\left(g(x,t)\bar{g}^{-1}(x,t) - I\right) \\ -g(x,t)\bar{g}^{-1}(x,t)\left[K_1\text{sat}(s_1/\xi_1) \ K_2\text{sat}(s_2/\xi_2) \ K_3\text{sat}(s_3/\xi_3) \right] \end{matrix} \right)^T \tag{15}$$

By choosing the positive and large enough values for K_1, K_2 and K_3, it can be shown that constraint of Eq. (8) would be satisfied. Then, the candidate Lyapunov function satisfies the Lyapunov stability criterion, which guarantees the asymptotic stability of the system. The terms $\bar{f}(x,t)$ and $\bar{g}(x,t)$ appear as the state vector $x(t)$ is replaced by $x(t) + \Delta x(t)$, which leads to add some uncertainty and unmodelled dynamics in the state space equations of the model.

$$\bar{u}_\delta = -K(\xi_i, \eta_i)\bar{e},$$
$$\bar{e} = \bar{x}_\delta - \bar{r}_\delta, \bar{r}_\delta = \bar{y}_R - \bar{y}^0 \tag{19}$$

where $K(\xi_i, \eta_i)$ is the feedback gain matrix, $\bar{e}$ is the error vector, $\bar{y}_R$ is the command vector signal that must be tracked. $\bar{y}^0 = [y_1^0 \ y_2^0 \ y_3^0]$ is the output vector, defined by Eqs. (1) and (2), at each operating point of Table 2. Substituting Eqs. (18) and (19) in the first derivative of Eq. (17), leads to the following equation:
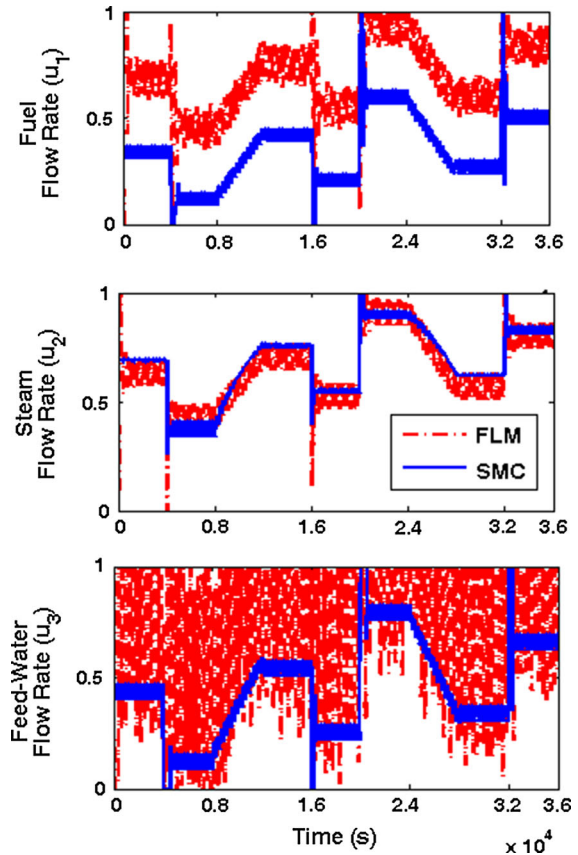
Fig. 10 Time response of the drum pressure (kg f/cm^2), electric output (MW), fluid density and drum water level in tracking a sequence of steps and ramps (case 'c' of Fig. 4) after implementation of sliding mode controller (*solid blue line*) and feedback linearization method (*dashed red line*); in the presence of Hopf bifurcation. (Color figure online)
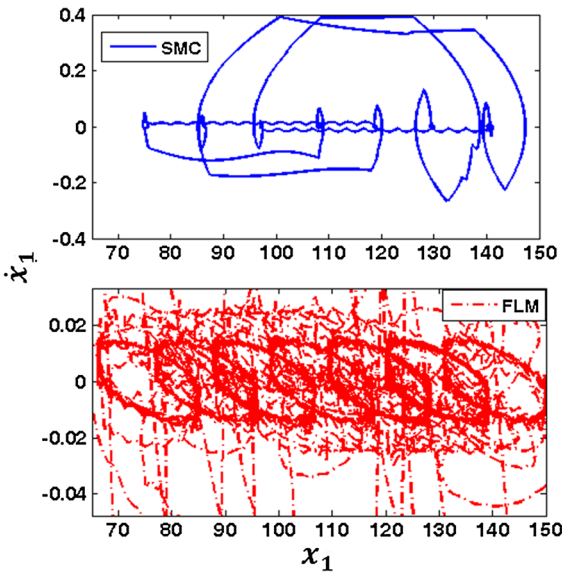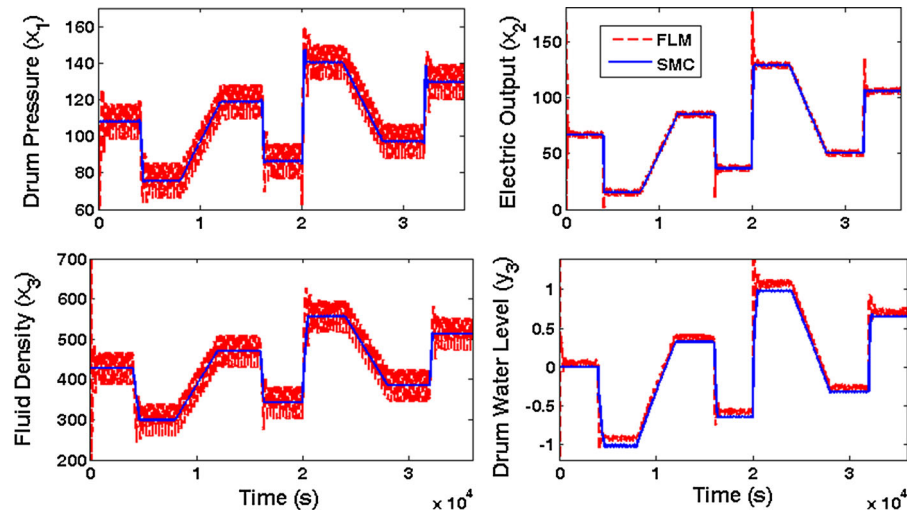
Fig. 11 Periodic and orbits of drum pressure (kg f/cm^2) in tracking a sequence of steps and ramps (case 'c'); after implementation of sliding mode controller (*solid blue line*) and feedback linearization method (*dashed red line*). (Color figure online)

$$\dot{\bar{x}}_\delta = [A - BK]\bar{x}_\delta + BK\bar{r}_\delta \qquad (20)$$

The procedure of designing a linear controller using feedback linearization method for the MIMO system is given in "Appendix." In the control design, a maximum overshoot of $M_p = 10\%$ and a settling time of about $t_s = 200$ s is considered as the desired output in tracking behavior of all output variables.

Fig. 12 Time response of the required fuel flow rate, u_1, steam flow rate, u_2, and feed-water flow rate, u_3, for the Hopf bifurcation control in tracking a sequence of steps and ramps (case 'c'); after implementation of sliding mode controller (*solid blue line*) and feedback linearization method (*dashed red line*). (Color figure online)

Fig. 13 Time response of
the drum pressure
(kg f/cm^2), electric output
(MW), fluid density and
drum water level in tracking
a sinusoidal signal (case 'd'
of Fig. 4) after
implementation of sliding
mode controller (*solid blue
line*) and feedback
linearization method
(*dashed red line*); in the
presence of Hopf
bifurcation. (Color figure
online)

Fig. 14 Periodic and quasi-periodic orbits of drum pressure
(kg f/cm^2) in tracking a sequence of a sinusoidal signal (case
'd'); after implementation of sliding mode controller (*solid blue
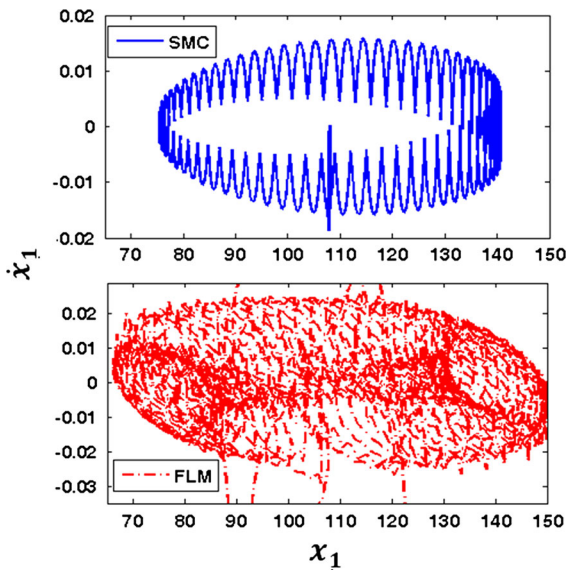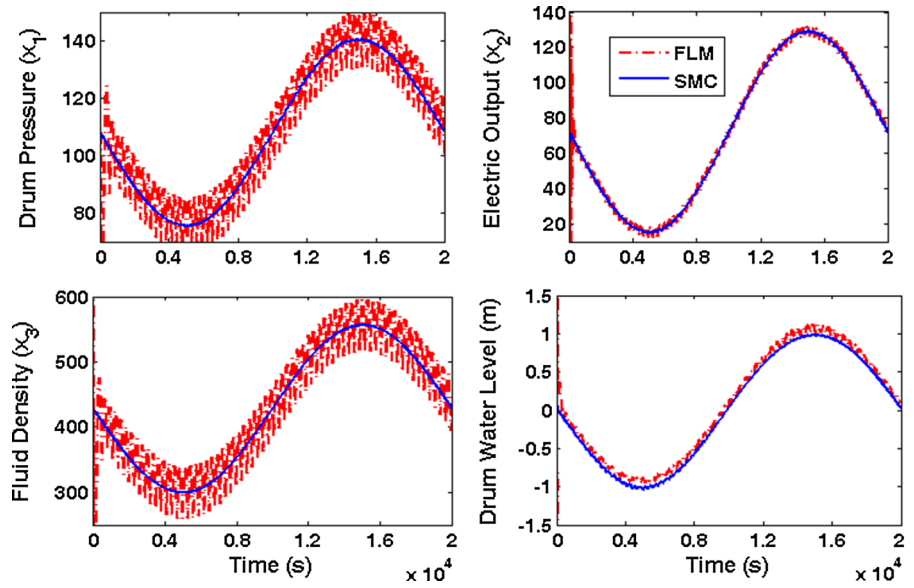line*) and feedback linearization method (*dashed red line*). (Color
figure online)

4 Simulations

In this section, nonlinear dynamics of the boiler–
turbine unit is simulated in the presence of harmonic
disturbances caused by environmental effects. If the
controller succeeds to reject these disturbances, it will

Fig. 15 Time response of the required fuel flow rate, u_1, steam
flow rate, u_2, and feed-water flow rate, u_3, for the Hopf bifur-
cation control in tracking a sinusoidal signal (case 'd'); after
implementation of sliding mode controller (*solid blue line*) and
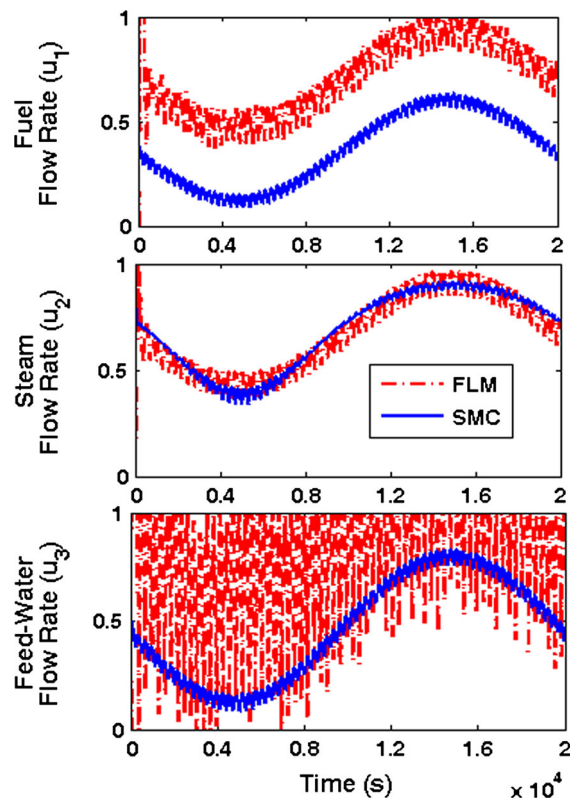feedback linearization method (*dashed red line*). (Color figure
online)

reject other kinds of transient disturbances, as they can be built up by the Fourier series. Realistic parameters of the model around the nominal operating point #4 are considered as the initial condition of the boiler–turbine unit as:

$$\Delta x_1 = 10 \sin 0.021t; \quad \Delta x_2 = 6 \sin 0.021t;$$
$$\Delta x_3 = 40 \sin 0.021t \tag{21}$$

To achieve the appropriate responses in tracking objectives while the control inputs are bounded in the acceptable ranges, parameters of the sliding mode controller are chosen by trial-and-error method as:

$$K_1 = K_2 = K_3 = 1; \quad \xi_1 = 10, \xi_2 = \xi_3 = 1 \tag{22}$$

In order to demonstrate the efficiency of designed controllers in switching between various operating points #1–#7 (Table 2), different arbitrary cases of the desired set-paths are assigned for the state variables: drum pressure, electric output, and fluid density. As shown in Fig. 3, a sequence of steps, ramps steps and a combination of them are considered as cases 'a', 'b', and 'c', respectively. Also, in order to investigate the ability of tracking of any arbitrary command, a sinusoidal command with variable amplitude is considered as case 'd.'

5 Results and discussion

5.1 case 'a'

The time response of the state variables: drum pressure ($x_1 = y_1$), electric output ($x_2 = y_2$), fluid density ($x_3 = y_3$) and drum water level in tracking a desired sequence of steps are shown in Fig. 4 (case 'a' in Fig. 3), after the implementation of SMC and FLM controllers. As it is observed, both controllers satisfy the tracking objective. But the FLM controller cannot eliminate the effect of unstable quasiperiodic solutions, arisen by Hopf bifurcation occurrence effectively. However, SMC controller regulates the unstable quasiperiodic solutions with large oscillations around the desired operating points.

Related limit cycles' behavior is shown in Fig. 5. As shown, although limit cycles exist in the time responses, FLM controller changes the large quasiperiodic limit cycles into the small periodic ones. On the other hand, limit cycles are vanished by using SMC controller. It

should be noticed that, the size of small diameter of elliptical limit cycles indicates the amount of oscillations around the operating points. As shown in Fig. 5, SMC controller is more effective rather than FLM one in maintaining the system around its operating points with small oscillatory behavior (equilibrium points are the final destinations in plots of top Fig. 5 for SMC).

Figure 6 shows the required variation of valve positions for the fuel (u_1), steam (u_2) and feed-water (u_3) flow rates for the purpose of bifurcation control in tracking of case 'a'. As it is observed, less amount of control efforts is required when the SMC controller is used (in comparison with FLM controller).

5.2 Cases 'b','c' and 'd'

Time responses and corresponding limit cycles of the drum pressure and electric output in tracking the desired paths of ramps steps (case 'b' in Fig. 3) are shown in Figs. 7 and 8, respectively. As shown, FLM controller is able to change the unstable quasiperiodic behavior of the system into a stable periodic one (around the fixed points). However, it cannot eliminate the oscillatory behavior in the tracking of the desired commands. But, SMC controller is capable of suppressing limit cycles. Also, required control efforts for bifurcation control and maintaining the system around the desired set-path of case 'b' are shown in Fig. 9. It is observed that when SMC controller is implemented, required control efforts are smoother (in comparison with the FLM controller).

Dynamic behavior of the boiler–turbine unit, in tracking a desired combination of ramps and steps (case 'c' of Fig. 3), is shown in Figs. 10, 11 and 12. As it is shown in Figs. 10 and 11, similar to the previous cases 'a' and 'b'; implementation of SMC controller leads to the efficient performance in the suppression of unstable quasiperiodic orbits. Moreover, less manipulation of valves positions for the fuel, steam and feed-water flow rates is required when SMC controller is used (Fig. 12). As another remark in all three cases, when SMC controller is used, oscillatory behavior is not observed for the output (as shown in Figs. 4, 7 and 10). This is more desirable for the power grid where less oscillations of the electric output around the desired operating points are expected.

Dynamic behavior of the boiler–turbine unit, in tracking a desired sinusoidal command with variable

amplitude (case 'd' of Fig. 3), is shown in Figs. 13, 14 and 15. Results show the good performance of both controllers. However, sliding mode controller leads to a better performance of the system. SMC leads to the lower amplitude variation around the operating point. Also, overshoots in this method are smaller compared with the FLM.

6 Conclusions

In this paper, control of nonlinear dynamics of a multi-input multi-output model of boiler–turbine unit is investigated in the presence of harmonic disturbances. Under bifurcation conditions which lead to the unstable quasiperiodic behavior of the output variables, implementation of an efficient controller is necessary. To track the desired paths for the state variables and consequently the water drum level, one linear (based on feedback linearization method, FLM) and one nonlinear controller (based on sliding mode control, SMC) are designed and applied on this nonlinear model. Their performance in suppression of perturbations and bifurcation control is compared.

Designed controllers guarantee the appropriate tracking performance of the boiler–turbine unit, against possible harmonic disturbances. While both controllers satisfy the constraint conditions on the control efforts, they result in smaller oscillatory behavior of limit cycles. This behavior is more obvious in the results of SMC. Moreover, SMC leads to the more smooth responses with less overshoots. Consequently, more stable electric output with very small oscillations is delivered to the power grid which is highly desired. On the other hand, when the SMC is applied, less control efforts with more smooth signals are predicted (which is the other great advantage of SMC in comparison with FLM).

Finally, it should be mentioned that the objective of bifurcation control is to decrease the effects of perturbations. According to the results, two different control approaches are examined in tracking of the desired commands. Also, their effectiveness to diminish the effects of unstable quasiperiodic behavior of the output variables is investigated. In other words, in the presence of bifurcations (due to nonlinear nature of the problem), the proposed controllers make the dynamic system to move from the unstable quasiperiodic responses into the stable periodic ones.

Appendix: Structure of the feedback control law in MIMO system

Dynamic model of the boiler–turbine unit is of rank $n = 3$. Since the controllability matrix

$$\mathbb{C} = [B \quad AB \quad A^2B \quad \ldots \quad A^{n-1}B]$$

is of rank 3, dynamic system is completely state controllable. Using the similarity transformation $\Re$ as $\bar{x} = \Re\bar{z}$, Eq. (17) is represented as:

$$\dot{\bar{z}}_\delta = \hat{A}_G\bar{z}_\delta + \hat{B}_G\bar{u}_\delta$$
$$\hat{A}_G = \Re^{-1}A\Re, \quad \hat{B}_G = \Re^{-1}B \tag{23}$$

where $\bar{z}_\delta$ is the new introduced state vector. Also, using the following transformations:

$$\bar{u}_\delta = F\bar{w}_\delta; \quad \bar{w}_\delta = \bar{v}_\delta - P\bar{z}_\delta \tag{24}$$

Equation (23) is described as:

$$\dot{\bar{z}}_\delta = A_G\bar{z}_\delta + B_G\bar{v}_\delta$$
$$A_G = \hat{A}_G - \hat{B}_GFP, \quad B_G = \hat{B}_GF \tag{25}$$

where $\bar{v}_\delta$ is the new control input vector and A_G, B_G has the general canonical form with elements of $[A_i]_{\gamma_i \times \gamma_i}$, $[B_i]_{\gamma_i \times 1}$, $i = 1, 2, .., r$ and $\sum_{i=1}^{r} \gamma_i = n$ as [34]:

$$A_G = \begin{bmatrix} [A_1] & 0 & \ldots & 0 \\ 0 & [A_2] & \ldots & 0 \\ & & . & \\ 0 & 0 & \ldots & [A_r] \end{bmatrix}_{n \times n},$$

$$B_G = \begin{bmatrix} [B_1] & 0 & \ldots & 0 \\ 0 & [B_2] & \ldots & 0 \\ & & . & \\ 0 & 0 & \ldots & [B_r] \end{bmatrix}_{n \times r},$$

$$[A_i] = \begin{bmatrix} 0 & 1 & 0 & \ldots & 0 \\ 0 & 0 & 1 & \ldots & 0 \\ & & & . & \\ 0 & 0 & 0 & \ldots & 1 \\ 0 & 0 & 0 & \ldots & 0 \end{bmatrix}_{\gamma_i \times \gamma_i},$$

$$[B_i] = \begin{bmatrix} 0 \\ 0 \\ . \\ . \\ 1 \end{bmatrix}_{\gamma_i \times 1} \tag{26}$$

where r is the number of input variables (in this case, $r = 3$). Introducing the modified controllability matrix as:

$$\bar{\mathbb{C}} = [b_1 \quad b_2 \quad .. \quad b_r \vdots Ab_1 \quad Ab_2 \quad .. \quad Ab_r \vdots ..... \vdots$$
$$A^{n-r}b_1 \quad A^{n-r}b_2 \quad .. \quad A^{n-r}b_r]$$

where b_i are the columns of matrix B given by Eq. (6); regular basis of $\bar{}$ is developed as

$$\hat{\mathbb{C}} = [\, b_1 \quad Ab_1 \quad .. \quad A^{\gamma_1-1}b_1 \,\vdots\, b_2 \quad Ab_2 \quad .. \quad A^{\gamma_2-1}b_2$$

$$\vdots \,.....\, \vdots\, b_r \quad Ab_r \quad .. \quad A^{\gamma_r-1}b_r\,] \tag{27}$$

where each column, $A^j b_i, i = 1, ldots, r, j = 0, \ldots, r$, is independent from its previous columns. Inverse of $\hat{\mathbb{C}}$ given by Eq. 27 is displayed as ([ ]$'$ stands for transpose of the [ ] quantity):

$$\hat{\mathbb{C}}^{-1} = \left[e'_{11} .. e'_{1\gamma_1} \,\vdots\, e'_{21} .. e'_{2\gamma_2} \,\vdots\, ... \,\vdots\, e'_{r1} .. e'_{r\gamma_r} \right]'$$

Similarity transformation $\Re$ is defined as [34]:

$$\Re = \left(\left[e'_{1\gamma_1}\, e'_{1\gamma_1}A, .. \, e'_{1\gamma_1}A^{\gamma_1-1} \,\vdots\, e'_{2\gamma_2}\, e'_{2\gamma_2}A .. \, e'_{2\gamma_2}A^{\gamma_2-1} \,\vdots\, ... \,\vdots\, e'_{r\gamma_r}\, e'_{r\gamma_r}A .. \, e'_{r\gamma_r}A^{\gamma_r-1} \right]' \right)^{-1} \tag{28}$$

Considering again Eq. 25 and constructing the feedback control law as $v_\delta = -\Gamma z_\delta$, yields:

$$\dot{\bar{z}}_\delta = A_{\mathrm{d}} \bar{z}_\delta,\ A_{\mathrm{d}} = A_{\mathrm{G}} - B_{\mathrm{G}}\Gamma \tag{29}$$

where A_{d} is the desired state matrix including coefficients representing the desired closed-loop poles ($|sI - A_{\mathrm{d}}| = (s - \mu_1)(s - \mu_2)...(s - \mu_n)$); having the general form of A_{G} as given by Eq. (26). Considering Eqs. (19), (24) and similarity transformation $\bar{x}_\delta = \Re \bar{z}_\delta$, yields the feedback control law of the system as:

$$\bar{u}_\delta = -K(\xi_i, \eta_i)\bar{x}_\delta$$

$$K(\xi_i, \eta_i) = F[\Gamma + P]\Re^{-1} \tag{30}$$

where F, P and Γ are obtained using Eqs. (24), (25) and (29) as follows:

$$F = (B'_{\mathrm{G}}\hat{B}_{\mathrm{G}})^{-1},\ P = B'_{\mathrm{G}}(A_{\mathrm{G}} - \hat{A}_{\mathrm{G}}),\ \Gamma$$
$$= B'_{\mathrm{G}}(A_{\mathrm{G}} - A_{\mathrm{d}}) \tag{31}$$

References

1. Tan, W., Marquez, H.J., Chen, T., Liu, J.: Analysis and control of a nonlinear boiler–turbine unit. J. Process Control **15**, 883–891 (2005)
2. Moradi, H., Bakhtiari-Nejad, F., Saffar-Avval, M.: Robust control of an industrial boiler system; a comparison between two approaches: sliding mode control & H_∞ technique. Energy Convers. Manag. **50**, 1401–1410 (2009)
3. Kouadri, A., Namoun, A., Zelmat, M.: Modelling the nonlinear dynamic behaviour of a boiler–turbine system using a radial basis function neural network. Int. J. Robust Nonlinear Control (2013). doi:10.1002/rnc.2969
4. Astrom, K.J., Bell, R.D.: Drum-boiler dynamics. Automatica **36**, 363–378 (2000)
5. Li, C., Zhou, J., Li, Q., An, X., Xiang, X.: A new T–S fuzzy-modeling approach to identify a boiler–turbine system. Expert Syst. Appl. **37**(3), 2214–2221 (2010)
6. Liu, X.J., Kong, X.B., Hou, G.L., Wang, J.H.: Modeling of a 1000 MW power plant ultra super-critical boiler system using fuzzy-neural network methods. Energy Convers. Manag. **65**, 518–527 (2013)
7. Astrom, K.J., Eklund, K.: A simplified nonlinear model of a drum boiler turbine unit. Int. J. Control **16**(1), 145–169 (1972)
8. Lo, K.L., Zeng, P.L., Marchand, E., Pinkerton, A.: Modelling and state estimation of power plant steam turbines. IEEE Proc. **137**(2), 80–94 (1990)
9. Murty, V.V., Sreedhar, R., Fernandez, B., Masada, G.Y., Hill, A.S.: Boiler system identification using sparse neural networks. In: Proceeding of Advances in Robust and Nonlinear Control Systems, ASME Winter Meeting, New Orleans, LA, USA, Article # 53, pp. 103–112 (1993)
10. Donate, P.D., Moiola, J.L.: Model of a once-through boiler for dynamic studies. Latin Am. Appl. Res. **24**, 159–166 (1994)
11. Moon, U.C., Lee, K.Y.: A boiler-turbine system control using a fuzzy auto-regressive moving average (FARMA) model. IEEE Trans. Energy Convers. **18**(1), 142–148 (2003)
12. Moradi, H., Alasty, A., Vossoughi, G.: Nonlinear dynamics and control of bifurcation to regulate the performance of a boiler–turbine unit. Energy Convers. Manag. **68**, 105–113 (2013)
13. Chen, D., Ding, C., Do, Y., Ma, X., Zhao, H., Wang, Y.: Nonlinear dynamic analysis for a Francis hydro-turbine governing system and its control. J. Frankl. Inst. Eng. Appl. Math. **351**(9), 4596–4618 (2014)
14. McDonald, J.P., Kwatny, H.G.: Design and analysis of boiler–turbine–generator controls using linear optimal regulator theory. IEEE Trans. Autom. Control AC **18**, 202 (1973)
15. Corit, R., Maffezzoni, C.: Practical-optimal control of a drum boiler power plant. Automatica **20**(2), 163–173 (1984)
16. Borsi, L.: Design and Experimental Evaluation of Decoupling Control for a Boiler Turbine Unit. Modelling and Control Seminar, Sidney (1977)
17. Prasad, G., Swidenbank, E., Hogg, B.W.: A Local model networks based multivariable long-range predictive control strategy for thermal power plants. Automatica **34**(10), 1185–1204 (1998)
18. Li, Y., Shen, J., Lee, K.Y., Liu, X.: Offset-free fuzzy model predictive control of a boiler–turbine system based on genetic algorithm. Simul. Model. Pract. Theory **26**, 77–95 (2012)

19. Prokhorenkov, A.M., Sovlukov, A.S.: Fuzzy models in control systems of boiler aggregate technological processes. Comput. Stand. Interfaces **24**, 151–159 (2002)

20. Kocaarslan, I., Ertuğrul, C., Tiryaki, H.: A fuzzy logic controller application for thermal power plants. Energy Convers. Manag. **47**, 442–458 (2006)

21. Liu, X.J., Lara-Rosanoa, F., Chan, C.W.: Neurofuzzy network modelling and control of steam pressure in 300 MW steam-boiler system. Eng. Appl. Artif. Intell. **16**, 431–440 (2003)

22. Chen, P.C., Shamma, J.S.: Gain-scheduled l^1-optimal control for boiler–turbine dynamics with actuator saturation. Process Control **14**, 263–277 (2004)

23. Fang, F., Wei, L.: Backstepping-based nonlinear adaptive control for coal-fired utility boiler–turbine units. Appl. Energy **88**, 814–824 (2011)

24. Moon, U.C., Lee, K.Y.: An adaptive dynamic matrix control with fuzzy-interpolated step-response model for a DRUM-type boiler-turbine system, no. 5738323. IEEE Trans. Energy Convers. **26**(2), 393–401 (2011)

25. Pellegrinetti, G., Bentsman, J.: H_∞ controller design for boilers. Int. J. Robust Nonlinear Control **4**, 645–671 (1994)

26. Tan, W., Marquez, H.J., Chen, T.: Multivariable robust controller design for a boiler system. IEEE Trans. Control Syst. Technol. **10**(5), 735–742 (2002)

27. Moradi, H., Saffar-Avval, M., Bakhtiari-Nejad, F.: Sliding mode control of drum water level in an industrial boiler unit with time varying parameters: A comparison with H-infinity robust control approach. J. Process Control **22**, 1844–1855 (2012)

28. Zheng, K., Bentsman, J., Taft, C.W.: Full operating range robust hybrid control of a coal-fired boiler/turbine unit. J. Dyn. Syst. Meas. Control Trans. ASME **130**(4), 111–114 (2008)

29. Moradi, H., Vossoughi, G., Alasty, A.: Suppression of harmonic perturbations and bifurcation control in tracking objectives of a boiler-turbine unit in power grid. Nonlinear Dyn. **76**(3), 1693–1709 (2014)

30. Tan, W., Fang, F., Tian, L., Fu, C., Liu, J.: Linear control of a boiler–turbine unit: analysis and design. ISA Trans. **47**, 189–197 (2008)

31. Bell, R.D., Astrom, K.J.: Dynamic models for boiler–turbine–alternator units: data logs and parameter estimation for a 160 MW unit. In: Technical Report Report LUTFD2/(TFRT-3192)/1-137; Department of Automatic Control, Lund Institute of Technology, Lund, Sweden (1987)

32. Moradi, H., Bakhtiari-Nejad, F.: Improving boiler unit performance using an optimum robust minimum-order observer. Energy Convers. Manag. **52**(3), 1728–1740 (2011)

33. Chen, D., Zhang, R., Ma, X., Liu, S.: Chaotic synchronization and anti-synchronization for a novel class of multiple chaotic systems via a sliding mode control scheme. Nonlinear Dyn. **69**(1–2), 35–55 (2012)

34. D'Azzo, J., Houpis, H.: Linear Control System Analysis and Design: Conventional and Modern, 4th edn. McGraw-Hill, New York (1995)